Core filling of dark solitons in a topological superfluid with one-dimensional spin-orbit coupling

Xinwei Fan,[1,*] Xin Zhang,[1] Zhongzhou Ren,[2,†] and Chang Xu[1]
[1]*School of Physics, Nanjing University, Nanjing 210093, China*
[2]*School of Physics Science and Engineering, Tongji University, Shanghai 200092, China*

(Received 9 February 2018; revised manuscript received 12 July 2018; published 16 January 2019)

We investigated the core-filling properties of dark solitons in one-dimensional spin-orbit-coupled Fermi gases. Majorana fermions can exist at the edges of the topological superfluid, when the spin-orbit coupling drives this system from the superfluid to the topological superfluid. Our results show that when dark solitons participate, the state of the system and the existence of Majorana zero-energy modes at the edges of topological superfluid correlate with the filling status of the core of the dark soliton. Furthermore, this dark soliton can actually accommodate two extra Majorana excitations without interactions in its core, when it is filled with highly imbalanced spins in a specific region of parameters. These features can be utilized to manipulate Majorana fermions in the topological superfluid.

DOI: 10.1103/PhysRevA.99.013612

I. INTRODUCTION

Solitons, like dark solitons or bright solitons, have exotic properties because of their nonlinearity, which can resist dispersion during propagation. They have been proved to be of great importance in many physical branches [1]. In ultracold atomic gases, dark solitons can be created by phase imprinting [2] or rapid quenches during the collisions of condensates [3,4]. Apart from their ubiquitous properties, which have been investigated extensively in theories [5–7] and experiments [8–12], there are some other interesting phenomena arising from the so-called topological superfluid [13,14] in the presence of spin-orbit coupling [13,15,16]. It is well known that with high spin imbalance, superfluid systems can be driven into an inhomogeneous Fulde-Ferrell-Larkin-Ovchinnikov (FFLO) phase [17–19] in low dimensions. However, when the spin-orbit coupling comes into play, the FFLO state will be suppressed and the system will be driven into a topological superfluid phase, where dark solitons can exist, in contrast to the FFLO state. It has been reported that Majorana zero-energy modes can exist in this topological superfluid because of its topological properties [20,21]. In this article, we present a more exotic phenomenon: that the existence of Majorana excitations at the edges of the topological superfluid is relevant to the filling status of the core of the dark soliton. When this dark soliton is filled, there are two extra Majorana excitations that coexist in the core without interactions. These results are in agreement with prior works [22,23]. Allowing for the fact that Majorana fermions have been proved to be promising candidates for quantum bit (qubit) for quantum computing because of its non-Abelian statistic property [24,25], these discoveries indeed establish relations between condensed-matter physics and the development of quantum computing.

In this article, we indicate that the state of the system and the existence of Majorana fermions at the edges of the topological superfluid are related to the filling status of the core of the dark soliton. Since a dark soliton is a diplike structure in the diagram of atomic density, the depth of this dip is controllable by adjusting parameters such as the strength of spin-orbit coupling, interatomic interaction, and external Zeeman field. When we change the depth of a dark soliton, it is equivalent to filling it with atoms. We show that we can control which kind of spin (up or down) fills in the soliton by carefully adjusting the parameters. More important, we find that only when filled with spin which is superior in total numbers in a specific region of parameters can two pairs of Majorana fermions exist at the edges of topological superfluid. However, if we increase the strength of spin-orbit coupling and Zeeman field to a special region, one of the two pairs of Majorana excitations will disappear and an extra pair of Majorana excitations will emerge in the core of the dark soliton. Compared with prior works done by several groups [22,23,26], our work specifies the relation between the existence of two kinds of Majorana excitations and the filling status of the core of the dark soliton.

There are articles [27,28] pointing out that the intrinsic instability of dark solitons could be suppressed by filling the core of solitons with imbalanced spins. This result holds even for soliton trains [27]. In this case, our research in fact gives insight into manipulating Majorana fermions carried by dark solitons which exist in the topological superfluid in high dimensions.

This article is arranged as follows. In Sec. II, we introduce our model based on the Bogoliubov–de Gennes (BdG) equation, which is derived from the mean-field theory. Although this model is a qualitative theory, it still captures most features of the system during the crossover from Bose-Einstein condensate (BEC) to Bardeen-Cooper-Schrieffer (BCS) superfluid [29]. In Sec. III, we will discuss thoroughly the relation between the existence of Majorana excitations and the filling

*fxinwei123@gmail.com
†zren@tongji.edu.cn

status in the the core of the dark soliton. In Sec. IV, a summary discussion and conclusion will be presented.

II. METHODOLOGY

The system is trapped in a two-dimensional optical lattice in the y-z plane; thus, it can be treated as a one-dimensional system. The spin-orbit coupling can be engineered by two Raman lasers propagating in the x and $-x$ directions [30,31]. The Hamiltonian of this system should be written in the form of second quantization:

$$H = \int dx \hat{\Psi}^\dagger(x) \mathscr{H}_s \hat{\Psi}(x) + H_I, \tag{1}$$

where $\hat{\Psi}(x) = [\hat{\Psi}_\uparrow(x), \hat{\Psi}_\downarrow(x)]^T$ and $\hat{\Psi}^\dagger(x) = [\hat{\Psi}^\dagger_\uparrow(x), \hat{\Psi}^\dagger_\downarrow(x)]$ are two-component spinors. $\hat{\Psi}^\dagger_\nu(x)$ and $\hat{\Psi}_\nu(x)$ denote the creation and annihilation operator of atoms respectively with a spin ν ($\uparrow$, $\downarrow$). The single-particle Hamiltonian $\mathscr{H}_s$ reads

$$\mathscr{H}_s = -\frac{\hbar^2}{2m}\frac{\partial^2}{\partial x^2} - \mu + V(x) + \alpha \hat{k}_x \sigma_y - h\sigma_z, \tag{2}$$

where the first term is the kinetic energy and m is the mass of atoms. The second term μ denotes the chemical potential, which has absorbed the recoil energy $E_L = \hbar^2 k_L^2/2m$ of the Raman laser. The external harmonic potential is $V(x) = m\omega^2 x^2/2$ with an oscillation frequency ω. The fourth term is the energy of spin-orbit coupling with the momentum operator $\hat{k}_x = -i\partial/\partial x$. $\alpha \equiv \hbar^2 k_L/m$ stands for the strength of spin-orbit coupling with a recoil momentum $\hbar k_L$ of the Raman laser. The last term denotes the energy shift caused by the Zeeman field originating from the Raman lasers, where $h = \hbar\Omega/2$ is the energy of the effective Zeeman field with a Rabi frequency Ω of the laser beam. σ_i are standard 2×2 Pauli matrices, where $i = x, y, z$.

The second term $H_I = g_{1D} \int dx \hat{\Psi}^\dagger_\uparrow(x)\hat{\Psi}^\dagger_\downarrow(x)\hat{\Psi}_\downarrow(x)\hat{\Psi}_\uparrow(x)$ on right side of Eq. (1) describes the interaction between two different spin states with an effective one-dimensional (1D) attractive interaction strength $g_{1D} = -2\hbar^2/ma_{1D}$. The 1D s-wave scattering length a_{1D} [32] originates from 3D scattering length a_{3D} [33], which can be tuned by Feshbach resonances in experiment. Here we introduce a dimensionless parameter $\gamma \equiv -mg_{1D}/n(0)\hbar^2$ to describe the interaction between atoms and fix it to $\gamma = 2.04$ in this article. This value can help us compare our result with that of previous work [23] when there is an overlap and it is accessible for experiments [33]. Note that it is an experimental parameter, which means it is supposed to be measured in the presence of the spin-orbit coupling. In this way, the effects of the spin-orbit coupling have been automatically included in this parameter, so we only need to focus on the single-particle Hamiltonian. There are theoretical works [34–36] that deal with the effects of the spin-orbit coupling on the two-body interaction. These results may help to get the exact form of the interactions between atoms in many-body system, but for now it is very convenient to adopt the experimental parameter. $n(0) = \sqrt{4Nm\omega/\hbar\pi^2}$ is the density of atoms at the center of the trap within Thomas-Fermi approximation. The number of atoms is $N = 80$ in our setup. Here we adopt the standard mean-field procedure to rewrite the interaction as

$$H_I \simeq -\int [\Delta(x)\Psi^\dagger_\uparrow(x)\Psi^\dagger_\downarrow(x) + \text{H.c.}]dx - \int dx \frac{|\Delta(x)|^2}{g_{1D}}, \tag{3}$$

where $\Delta(x) \equiv -g_{1D}\langle\Psi_\downarrow(x)\Psi_\uparrow(x)\rangle$ is the complex order parameter of the superfluid system in zero temperature. Now we can define a Nambu spinor $\psi(x) \equiv [\Psi_\uparrow(x), \Psi_\downarrow(x), \Psi^\dagger_\downarrow(x), \Psi^\dagger_\uparrow(x)]^T$ and rewrite our Hamiltonian in Eq. (1) as

$$H \simeq \int \left[\frac{1}{2}\psi^\dagger(x)\mathscr{H}_{\text{BdG}}\psi(x) - \frac{|\Delta(x)|^2}{g_{1D}}\right]dx + \text{Tr}\mathscr{H}_0, \tag{4}$$

where $\mathscr{H}_0 = -\frac{\hbar^2}{2m}\frac{\partial^2}{\partial x^2} - \mu + V(x)$ and $\text{Tr}\mathscr{H}_0$ is the trace of $\mathscr{H}_0$. We can write $\mathscr{H}_{\text{BdG}}$ in the form of 4×4 matrix:

$$\mathscr{H}_{\text{BdG}} = \begin{pmatrix} \mathscr{H}_s & -i\Delta(x)\sigma_y \\ i\Delta^*(x)\sigma_y & -\mathscr{H}_s^* \end{pmatrix}. \tag{5}$$

A. Bogoliubov–de Gennes (BdG) equation

According to the Bogoliubov transformation, we can diagonalize the BdG Hamiltonian in the following form,

$$\mathscr{H}_{\text{BdG}}\Phi_n(x) = E_n\Phi_n, \tag{6}$$

where $\Phi_n = [u_{\uparrow n}(x), u_{\downarrow n}(x), v_{\downarrow n}(x), v_{\uparrow n}(x)]^T$ and its conjugate $\Phi^*_n = [u^*_{\uparrow n}(x), u^*_{\downarrow n}(x), v^*_{\downarrow n}(x), v^*_{\uparrow n}(x)]^T$ are wave functions of particles and holes with energy E_n and $-E_n$, respectively, where $n = 1, 2, 3....$ We can express the order parameter $\Delta(x)$ by $u(x)$ and $v(x)$ as

$$\Delta(x) = -\frac{g_{1D}}{2}\sum_{|E_n|<E_c}[u_{\uparrow n}v^*_{\downarrow n}\Theta(E_n) + u_{\downarrow n}v^*_{\uparrow n}\Theta(-E_n)]. \tag{7}$$

Note that the Fermi distribution function $f(E_n) = 1/(e^{E_n/k_BT} + 1)$ here degenerates to the Heaviside step function $\Theta(E_n)$ since we are interested in the zero-temperature situation. Here the index of the summation means we only consider up to the nth energy level with corresponding energy E_n close to a cutoff E_c, and similarly hereafter. The high-energy cutoff $E_c \approx 560\hbar\omega$ is sufficient enough in our setup.

B. Numerical methods

The Bogoliubov–de Gennes (BdG) equation can be solved numerically with an iterative procedure and we will introduce our method briefly here. In order to solve Eq. (6), we need to know the exact form of $\Delta(x)$. However, to get the exact form of $\Delta(x)$, we have to solve Eq. (6). This is a typical self-consistent system, and we always handle this kind of system by iteration. First, we choose an initial ansatz $\Delta(x) = \Delta_0 \exp[i\pi\Theta(x - x_i)]$. The reason we choose this ansatz is that the order parameter will change its sign when going through a dark solion located at the point node x_i. It is equivalent to getting a π phase jump, and this form of order parameter can exactly capture this picture due to the property of the Heaviside function. It is worth noting that this expression may also be applicable when it comes

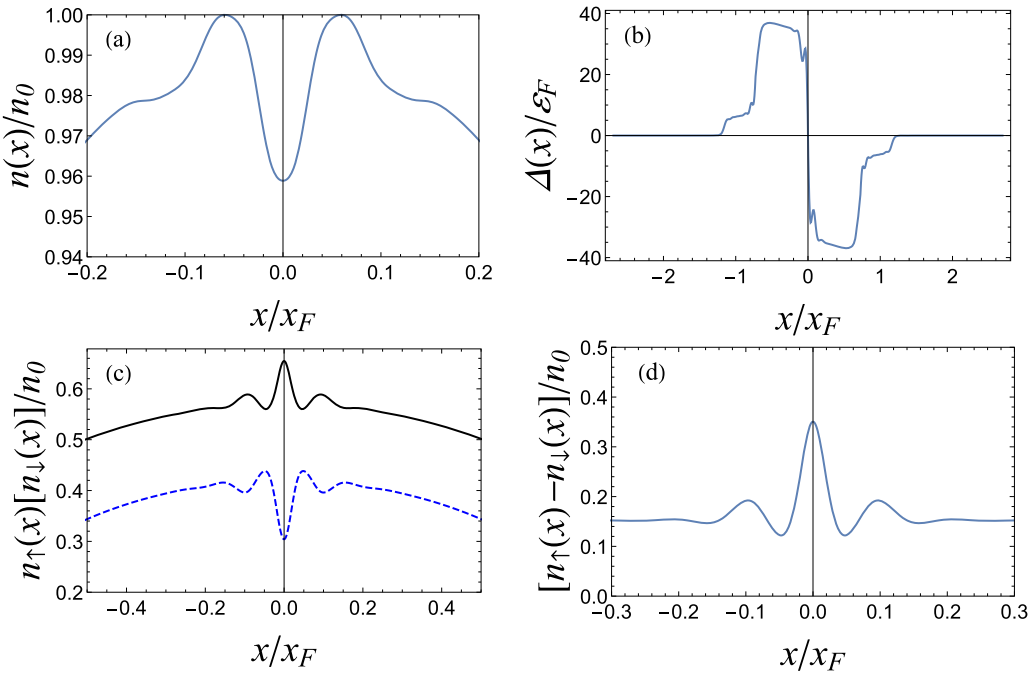

FIG. 1. (a) The typical diplike density plot of a dark soliton. (b) The profile of pairing energy gap $\Delta(x)$. We can see that $\Delta(x)$ plunges cross the origin which is the center location of the dark soliton. (c) The density distributions of up spins (solid line) and down spins (dashed line) near the core of the soliton. It is clear that up spins fill in the core of the soliton instead of the down spins. Their density difference near the core is shown in panel (d). n_0 is the maximum total density near the $x = 0$. The spin-orbit coupling strength and the Zeeman field are $\alpha = 0.6\epsilon_F/k_F$ and $h = 0.4\epsilon_F$, respectively.

to a multiple-soliton situation [22] if we want to manipulate soliton trains in the future.

Subsequently, we take this initial $\Delta(x)$ to Eq. (6) and solve the BdG equation by basis expansion. We implement $N_s = 300$ single-particle harmonic eigenstates to expand the $u(x)$ and $v(x)$, and then produce a new $\Delta(x)$. This procedure will not stop until $\Delta(x)$ converges to a stable value. Then we extract the $v(x)$ and $u(x)$ in $\Phi_n(x)$ with their corresponding

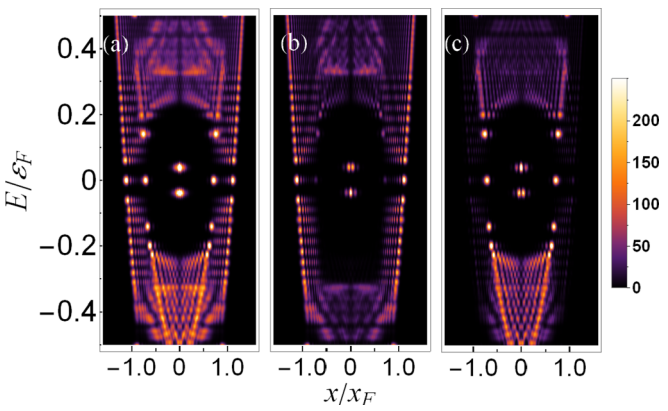

FIG. 2. (a) The total density of state $\rho(x, E)$ with two pairs of Majorana excitations located at the edges $x \approx \pm 1.1x_F$ and $x \approx \pm 0.7x_F$, respectively. Panels (b) and (c) indicate that the two pairs of Majorana excitations are contributed by $\rho_\uparrow(x, E)$ and $\rho_\downarrow(x, E)$ separately. $\rho_\sigma(x, E)$ is calculated with Eq. (8). Here the strength of spin-orbit coupling is $\alpha = 0.6\epsilon_F/k_F$ and the Zeeman field is $h = 0.4\epsilon_F$.

E_n. So far, since all ingredients are available here, we present our analysis in next section.

III. ANALYSIS

In this section, we try to reveal the relation between the existence of Majorana excitations and the different filling statuses of the core of the dark soliton. Without loss of generality, we have chosen the direction of the Zeeman field so that there are more up spins than down spins, i.e., $n_\uparrow > n_\downarrow$. As soon as we get the information about the eigenfunctions $u(x)$, $v(x)$, and their corresponding eigenvalues, we can calculate the local density of states

$$\rho_\sigma(x, E) = \frac{1}{2}\sum_{|E_n|<E_c}[|u_{\sigma n}|^2\delta(E - E_n) + |v_{\sigma n}|^2\delta(E + E_n)], \tag{8}$$

and the density of atoms

$$n_\sigma(x) = \langle\hat{\Psi}_\sigma^\dagger(x)\hat{\Psi}_\sigma(x)\rangle = \frac{1}{2}\sum_{|E_n|<E_c}[|u_{n\sigma}(x)|^2\Theta(E_n) + |v_{n\sigma}(x)|^2\Theta(-E_n)], \tag{9}$$

which satisfies the constraint $N = \int dx(n_\uparrow(x) + n_\downarrow(x))$. The typical density profile of a dark soliton and its order parameter are shown in Figs. 1(a) and 1(b). Figures 1(c) and 1(d) are characteristic patterns of imbalanced spins. The spin-orbit-coupling strength is $\alpha = 0.6\epsilon_F/k_F$ in Fig. 1, where the $k_F = \sqrt{2m\epsilon_F}/\hbar$ is the Fermi wave vector with the Fermi energy

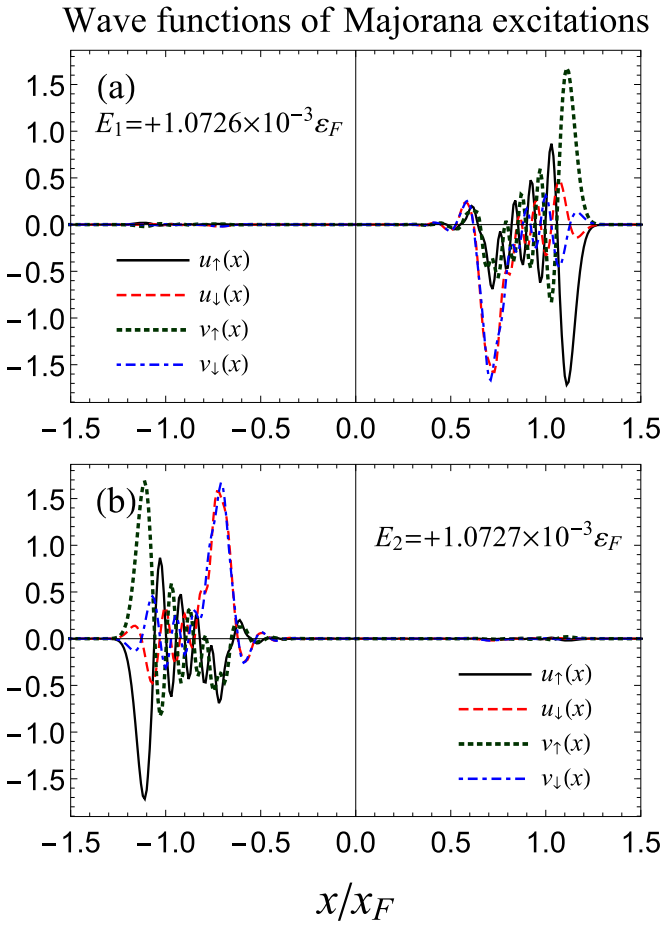

FIG. 3. Wave functions of Majorana excitations. The energy of the two Majorana excitations are very close: $E_1 = +1.0726 \times 10^{-3}$ in panel (a) and $E_2 = +1.0727 \times 10^{-3}$ in panel (b). Because of the symmetry of the BdG equation, there are two corresponding states which possess the same physical meaning but with negative energy. The strength of spin-orbit coupling is $\alpha = 0.6\epsilon_F/k_F$ and the Zeeman field is $h = 0.4\epsilon_F$.

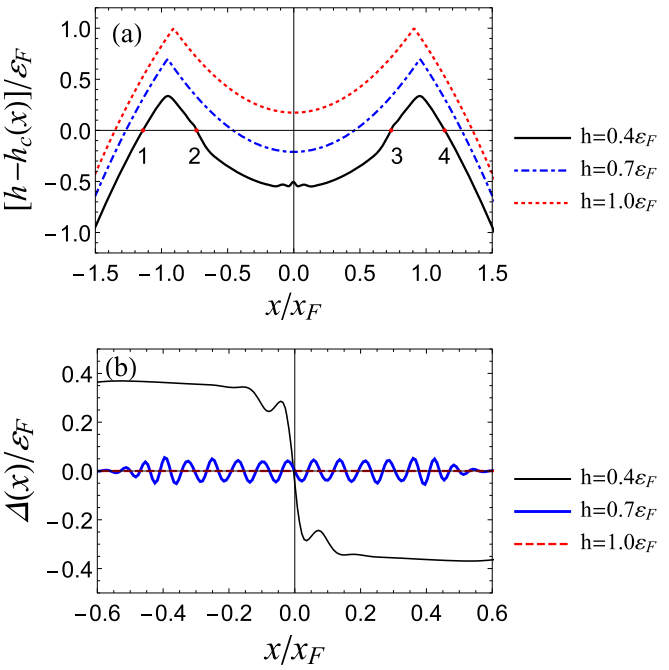

FIG. 4. (a) The critical Zeeman field $h - h_c(x)$. We can find that $h - h_c(x) > 0$ only at the wings, which means these regions are in topological superfluid states. The two pairs of Majorana excitations which exist at the edges of the topological regions are highlighted by red points. (b) The order parameters of three Zeeman fields. We can see that the order parameter oscillates drastically when increasing the Zeeman field to $h = 0.7\epsilon_F$ and is very small when $h = 1.0\epsilon_F$. Here $\alpha = 0.6\epsilon_F/k_F$.

$\epsilon_F = N\hbar\omega/2$, which is also used as the units of energy. The length coordinates are scaled by $x_F = \sqrt{N\hbar/m\omega}$. Figure 1(c) shows that a filling has happened in the core of the soliton for there is a bulge in the profile of up spins around $x = 0$, which means the atoms with up spins prefer to stay in the core of the soliton rather than the outside in contrast to the down spins. Figure 2 shows the local density of states $\rho_\uparrow(x, E)$, $\rho_\downarrow(x, E)$, and their summation $\rho(x, E)$ with the same parameters of Fig. 1. We find that Andreev fermionic bound states [5] are located in the core ($x \approx 0$) of the soliton and two pairs of Majorana excitations are located respectively at the edges of topological regions. Here we pair the Majorana excitations by their distance from the center, i.e., the inner and outer pair. However, from the aspect of energy, each side (left and right) of Majorana excitations occupies the same energy, which is shown by their wave functions in Fig. 3. The energies of these Majorana excitations are $|E_M| \approx 10^{-3}\epsilon_F$. The two pairs of Majorana modes emerge because the system has partially entered a topological superfluid phase [23], which means only the wings of the system are in the topological superfluid phase, while the center is still in a normal superfluid state. Here we adopt the local density approximation to justify this point.

It is known that there is a critical Zeeman field [37] $h_c = \sqrt{\mu^2 + \Delta^2}$ between the normal superfluid and topological superfluid. For a system which is normal (topological) superfluid, we have $h < h_c$ ($h > h_c$), but not vice versa, which will be addressed later. Allowing for the harmonic trap applied to the system, we can implement the local density approximation by changing the chemical potential μ to a local one $\mu(x) = \mu - V(x)$, and then the critical Zeeman field will be $h_c(x) = \sqrt{\mu^2(x) + \Delta^2(x)}$.

Figure 4(a) shows that in the condition ($h = 0.4$) of Fig. 2, the Zeeman field $h > h_c(x)$ only at the wings of the system, which makes these regions topological. Here we will show the limitation of the critical Zeeman field h_c. Increasing the Zeeman field h to a certain degree, say, $h = 0.7\epsilon_F$, we find that the order parameter in Fig. 4(b) oscillates drastically, which means the system has entered the FFLO superfluid state [26] instead of a topological state, even if h is still larger than $h_c(x)$ in some regions. At the same time, down spins accumulate around the core of the soliton instead of the up spins, even though they remain the superior ones. It will be more obvious if we increase the Zeeman field to $h = 0.9\epsilon_F$, as shown in Fig. 5. Majorana excitations will also disappear when down spins accumulate around the core, which is shown in Fig. 6. However, this trend will not last long. If we continue to increase h to $1.0\epsilon_F$, the order parameter will be extremely small, so the system can no longer be considered as a

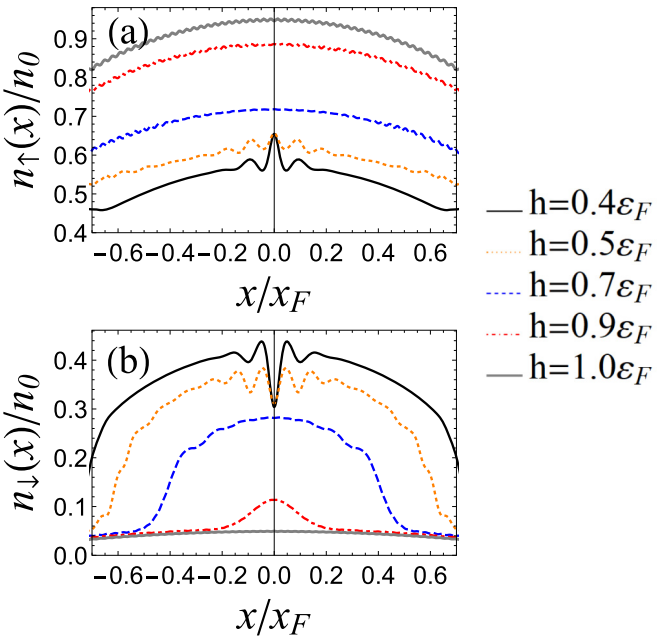

FIG. 5. (a) The distribution of up spins near the core of the dark soliton. We can see that with an increasing Zeeman field h, the up spins stop filling the core gradually. In contrast, panel (b) shows that the down spins start to accumulate around the core, especially when $h = 0.9$. However, the down spins will also stop gathering around the core if we continue increasing h. The strength of spin-orbit coupling is $\alpha = 0.6\epsilon_F/k_F$ here.

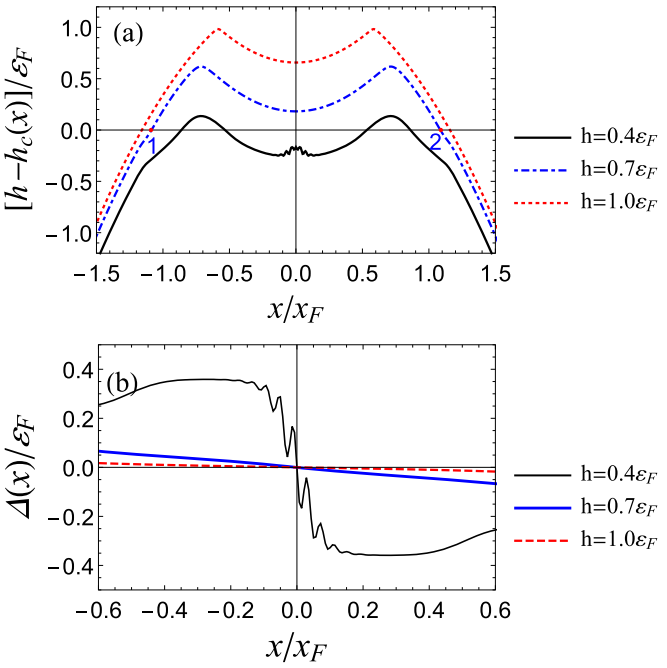

FIG. 7. (a) The critical Zeeman field $h - h_c(x)$. We can see that the region $x \in [-1.1, 1.1]$ is in topological superfluid state. Thus, only the outer pair of Majorana excitations remains at the edges (the red points in $h = 0.7\epsilon_F$). (b) The order parameters with different Zeeman fields. In contrast to the situation when $\alpha = 0.6\epsilon_F/k_F$ in Fig. 4(b), the order parameter will not oscillate, which means we can suppress the FFLO state with large strength of spin-orbit coupling. Here $\alpha = 1.3\epsilon_F/k_F$.

superfluid. Meanwhile, the down spins will stop gathering and the core of this soliton will be filled to a flat state corresponding to a quasihorizontal curve in the density diagram. The series of events suggest that the state of the system is relevant to the filling status of the core of the soliton.

Note that, in correlation with dark solitons though, those Majorana excitations shown in Fig. 2 can in fact exist without solitons [26,38]. In this case, dark solitons are more like an indictor of these Majorana excitations, which means we can

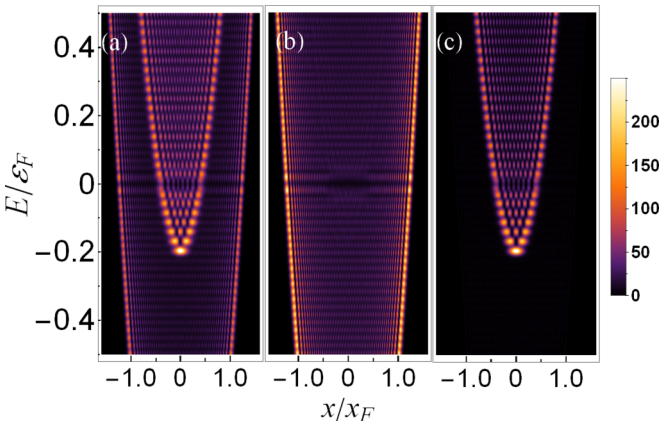

FIG. 6. Panels (a), (b), and (c) are the local densities of states $\rho(x, E)$, $\rho_\uparrow(x, E)$, and $\rho_\downarrow(x, E)$ respectively. In contrast to the situation with a smaller Zeeman field in Fig. 2, there is no sign of Majorana excitations. The up spins stop filling the core of the dark soliton at the same time (see Fig. 5). Here, $\alpha = 0.6\epsilon_F/k_F$ and $h = 0.7\epsilon_F$.

estimate the state of the system and the existence of Majorana excitations by the filling status of the dark soliton with specific parameters in the experiment.

However, there is another kind of Majorana excitations which is carried by the dark soliton in the topological superfluid. When we increase the strength of spin-orbit coupling above $\alpha = 1.2\epsilon_F/k_F$ and adjust the energy of Zeeman field to $h = 0.7\epsilon_F$, we find that the system will not evolve into the FFLO superfluid state but a full topological superfluid state. In this phase, the center of the system also satisfies the condition $h > h_c(x)$ as shown in Fig. 7(a). In contrast to the case of the FFLO state in Fig. 4(b), the order parameter will not oscillate in this topological phase, which is shown in Fig. 7(b). Since the whole region (between the two edges) is topological, the inner edges will disappear along with the inner pair of Majorana excitations. However, we also find that there is a cloudlike structure [22] emerging near $x = 0$, shown in Fig. 8(a). This structure near the core consists of two Majorana excitations with energy $|E_{M'}| \approx 10^{-6}\epsilon_F$. It is a result of the overlapping of the bound states [22,23], which means the energy of the two bound states will decrease close to zero in this topological phase. Compared with no soliton situation in Fig. 8(b), it is clear that these two Majorana excitations near $x = 0$ are indeed a consequence of the existence of the dark soliton. More specifically, it originates from the the bound states carried by the dark soliton [5,22]. Besides, the atoms fill the core of the dark soliton to a flat state as shown in Fig. 8(c) in this phase. Once again, the state of the system can

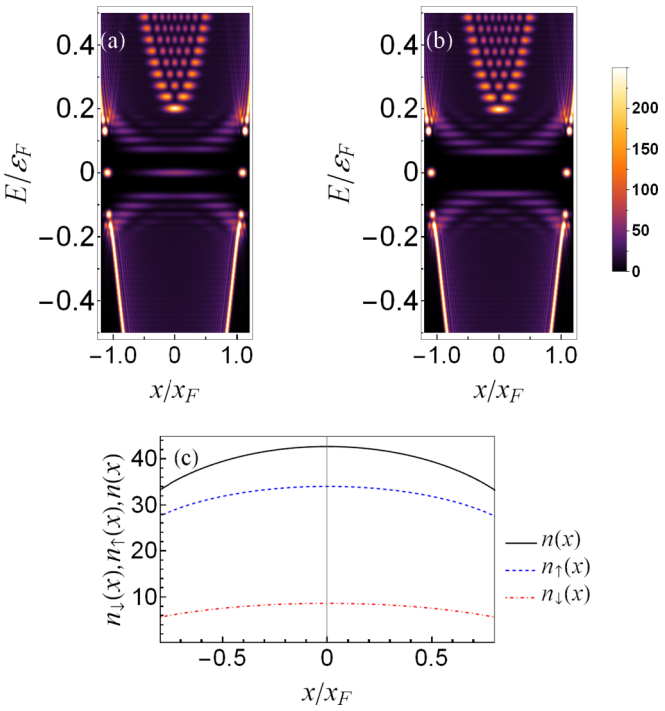

FIG. 8. Panel (a) is the local density of state when a dark soliton exists in the topological superfluid. Panel (b) is the local density of state without solitons. It is clear that panels (a) and (b) are nearly identical except for the Majorana excitations located at $x \approx 0$ in panel (a). So we confirm that this kind of Majorana excitations is carried by the dark soliton in contrast to the former kind in Fig. 2. We can see from the density distribution of atoms (c) that the core of the dark soliton in (a) is fully filled. Here $\alpha = 1.3\epsilon_F/k_F$ and $h = 0.7\epsilon_F$ for both situations.

be indicated by the filling status of the core, so is the existence of the Majorana excitations.

We present a region diagram of the filling status with different parameters in Fig. 9. This diagram is the essence of this work since the discussions above are merely examples of this diagram. Every region has two marks, character and color, which stand for the filling status of the core and the state of the system, respectively. First, the UF region with blue background means the core of the dark soliton is filled by up spins and the system is normal superfluid. There is a special region in the UF, namely the region in purple. It is a region that the filling status is still UF, but the system is partially topological; see Fig. 4. Since it is still in the UF region, the boundary is a dot-dashed line instead of a solid line. Second, the DF region with yellow background indicates the core is filled by the down spins and the system now is in the FFLO state. The FF region in green indicates the core is flatly filled, see Fig. 8(c), and the system is in a normal state, not a superfluid state. We notice that for $\alpha > 1.2\epsilon_F/k_F$ and to the range we have examined, the down spins will not participate in the filling process and the FFLO state will be suppressed by large strength of the spin-orbit coupling, which give rise to the last region, namely the FF region with orange. In there, the core is flatly filled, but the system is in a topological state and the dark soliton starts to carry its own Majorana excitations in its core, shown in Fig. 8(a).

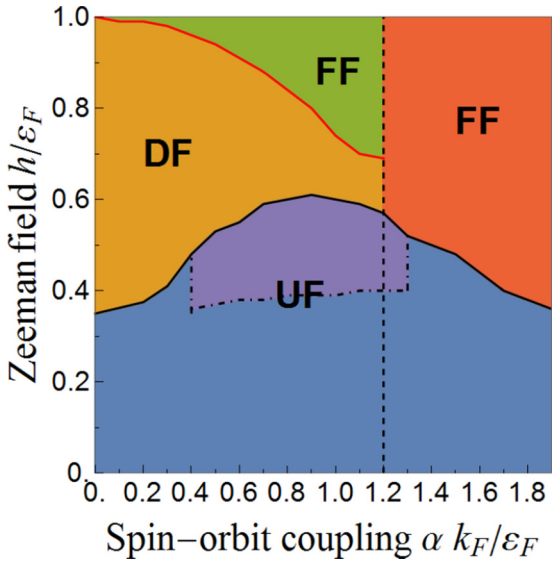

FIG. 9. The region diagram of the filling statuses. Different colors correspond to different state of the system where UF and DF denote that the core fills with up spins and down spins, respectively. FF denotes the region where the core is flatly filled. The system is partially topological in the purple part of the UF region and in there two pairs of Majorana excitations can exist at the edges of the topological superfluid. In the orange region, the dark soliton can carry two Majorana excitations in its core.

It is well known that dark solitons will suffer an intrinsic instability [6,39–41] when it comes to high dimensions. Recently, there are works [27,28] indicating that the instability can be suppressed when imbalanced spins fill the core of the soliton. The magnitude of the suppression is proportional to the degree of the imbalance, which means that the larger ratio of imbalanced spins the core possesses, the more stable the soliton will be. Here, we define the polarization as

$$P(x) = \frac{n_\uparrow(x) - n_\downarrow(x)}{n_\uparrow(x) + n_\downarrow(x)}. \tag{10}$$

In the orange region of Fig. 9, where the dark soliton can carry Majorana excitations in its core, the polarization is $P(0) \approx 0.5$, which is high enough to suppress the instability [28] if it can be maintained in high dimensions with time-dependent evolution. We hope it can be clarified further in the future because it may be a key to manipulating dark solitons or soliton trains which can carry Majorana excitations in the topological superfluid.

IV. DISCUSSION AND CONCLUSION

In this article, we show that the state of the system and the existence of Majorana fermions at the edges of the topological superfluid are related to the filling status of the core of the dark soliton. We point out that only in a specific region of parameters (purple part of Fig. 9) can two pairs of Majorana fermions exist at the edges of the topological superfluid. Furthermore, the dark soliton can carry its own Majorana excitations in the core with a high spin imbalance which could be utilized to suppress the instability of the dark soliton in high dimensions within the orange part of Fig. 9. Our

results also provide a possible way to search for the Majorana excitations and the FFLO state experimentally by detecting the density distribution of different spins around the core of the dark soliton. Considering that Majorana fermions have been proved to be a promising candidate for quantum bit for quantum computing, this work improves the maneuverability of Majorana fermions and the possibility of realizing quantum computing in the topological superfluid with the participation of solitons or soliton trains.

ACKNOWLEDGMENTS

This work is supported by the National Key R&D Program of China (Contracts No. 2018YFA0404403 and No. 2016YFE0129300), by the National Natural Science Foundation of China (Grants No. 11535004, No. 11761161001, No. 11375086, No. 11120101005, No. 11175085, No. 11235001, and No. 11881240623), and by the Science and Technology Development Fund of Macau under Grant No. 008/2017/AFJ.

[1] L. F. Mollenauer, R. H. Stolen, and J. P. Gordon, Phys. Rev. Lett. **45**, 1095 (1980); N. J. Zabusky and M. D. Kruskal, *ibid.* **15**, 240 (1965); A. J. Heeger, S. Kivelson, J. R. Schrieffer, and W. P. Su, Rev. Mod. Phys. **60**, 781 (1988).

[2] J. Denschlag, J. E. Simsarian, D. L. Feder, C. W. Clark, L. A. Collins, J. Cubizolles, L. Deng, E. W. Hagley, K. Helmerson, W. P. Reinhardt *et al.*, Science **287**, 97 (2000).

[3] G. Lamporesi, S. Donadello, S. Serafini, F. Dalfovo, and G. Ferrari, Nat. Phys **9**, 656 (2013).

[4] L. Khaykovich, F. Schreck, G. Ferrari, T. Bourdel, J. Cubizolles, L. D. Carr, Y. Castin, and C. Salomon, Science **296**, 1290 (2002).

[5] M. Antezza, F. Dalfovo, L. P. Pitaevskii, and S. Stringari, Phys. Rev. A **76**, 043610 (2007).

[6] A. M. Mateo and J. Brand, New J. Phys. **17**, 125013 (2015).

[7] A. Muryshev, G. V. Shlyapnikov, W. Ertmer, K. Sengstock, and M. Lewenstein, Phys. Rev. Lett. **89**, 110401 (2002).

[8] M. J. H. Ku, W. Ji, B. Mukherjee, E. Guardado-Sanchez, L. W. Cheuk, T. Yefsah, and M. W. Zwierlein, Phys. Rev. Lett. **113**, 065301 (2014).

[9] M. J. H. Ku, B. Mukherjee, T. Yefsah, and M. W. Zwierlein, Phys. Rev. Lett. **116**, 045304 (2016).

[10] X. Ma, O. A. Egorov, and S. Schumacher, Phys. Rev. Lett. **118**, 157401 (2017).

[11] S. Donadello, S. Serafini, M. Tylutki, L. P. Pitaevskii, F. Dalfovo, G. Lamporesi, and G. Ferrari, Phys. Rev. Lett. **113**, 065302 (2014).

[12] T. Yefsah, A. T. Sommer, M. J. H. Ku, L. W. Cheuk, W. Ji, W. S. Bakr, and M. W. Zwierlein, Nature (London) **499**, 426 (2013).

[13] M. Gong, S. Tewari, and C. Zhang, Phys. Rev. Lett. **107**, 195303 (2011).

[14] M. Z. Hasan and C. L. Kane, Rev. Mod. Phys. **82**, 3045 (2010).

[15] M. Gong, G. Chen, S. Jia, and C. Zhang, Phys. Rev. Lett. **109**, 105302 (2012).

[16] L. Han and C. A. R. Sá de Melo, Phys. Rev. A **85**, 011606 (2012).

[17] C. Chen, Phys. Rev. Lett. **111**, 235302 (2013).

[18] T. Paananen, J. Phys. B **42**, 165304 (2009).

[19] S. Dutta and E. J. Mueller, Phys. Rev. A **96**, 023612 (2017).

[20] S. L. Zhu, L. B. Shao, Z. D. Wang, and L. M. Duan, Phys. Rev. Lett. **106**, 100404 (2011).

[21] M. Sato, Y. Takahashi, and S. Fujimoto, Phys. Rev. Lett. **103**, 020401 (2009).

[22] X.-J. Liu, Phys. Rev. A **91**, 023610 (2015).

[23] Y. Xu, L. Mao, B. Wu, and C. Zhang, Phys. Rev. Lett. **113**, 130404 (2014).

[24] A. Kitaev, Phys. Usp. **44**, 131 (2001).

[25] A. Kitaev, Ann. Phys. N.Y. **321**, 2 (2006).

[26] X.-J. Liu and H. Hu, Phys. Rev. A **85**, 033622 (2012).

[27] S. Dutta and E. J. Mueller, Phys. Rev. Lett. **118**, 260402 (2017).

[28] M. D. Reichl and E. J. Mueller, Phys. Rev. A **95**, 053637 (2017).

[29] W. Z. M. Randeria and M. Zwierlein, *The BCS-BEC Crossover and the Unitary Fermi Gas*, edited by W. Zwerger, Lecture Notes in Physics Vol. 836 (Springer, Berlin, Heidelberg, 2012).

[30] P. Wang, Z. Q. Yu, Z. Fu, J. Miao, L. Huang, S. Chai, H. Zhai, and J. Zhang, Phys. Rev. Lett. **109**, 095301 (2012).

[31] L. W. Cheuk, A. T. Sommer, Z. Hadzibabic, T. Yefsah, W. S. Bakr, and M. W. Zwierlein, Phys. Rev. Lett. **109**, 095302 (2012).

[32] M. Olshanii, Phys. Rev. Lett. **81**, 938 (1998).

[33] Y. A. Liao, A. S. Rittner, T. Paprotta, W. Li, G. B. Partridge, R. G. Hulet, S. K. Baur, and E. J. Mueller, Nature (London) **467**, 567 (2010).

[34] R. Zhang and W. Zhang, Phys. Rev. A **88**, 053605 (2013).

[35] S. J. Wang, Q. Guan, and D. Blume, Phys. Rev. A **98**, 022708 (2018).

[36] Y. C. Zhang, S. W. Song, and W. M. Liu, Sci. Rep. **4**, 4992 (2014).

[37] Y. Oreg, G. Refael, and F. von Oppen, Phys. Rev. Lett. **105**, 177002 (2010).

[38] R. Wei and E. J. Mueller, Phys. Rev. A **86**, 063604 (2012).

[39] P. G. Kevrekidis, G. Theocharis, D. J. Frantzeskakis, and A. Trombettoni, Phys. Rev. A **70**, 023602 (2004).

[40] E. A. Kuznetsov and J. J. Rasmussen, Phys. Rev. E **51**, 4479 (1995).

[41] W. Wen, C. Zhao, and X. Ma, Phys. Rev. A **88**, 063621 (2013).